Fabrication of Metallic Magnetic Calorimeter X-ray Detector Arrays

W-T. Hsieh[a, *], J. A. Adams[a], S. R. Bandler[a], J. Beyer[b], K. L. Denis[a], H. Eguchi[c], E. Figueroa-Feliciano[d], H. Rotzinger[a], G. H. Schneider[a], G. M. Seidel[c], T. R. Stevenson[a], D. E. Travers[a]

[a]*NASA Goddard Space Flight Center, Greenbelt, MD 20771, USA*
[b] *Physikalisch-Technische Bundesanstalt, Institute Berlin, Abbes, 2-12, D-10587 Berlin, Germany*
[c]*Physics Department, Brown University, Providence, RI 02912, USA*
[d]*Physics Department, Massachusetts Institute of Technology, Cambridge, MA 02139, USA*
**Corresponding author: wen-ting.hsieh-1@nasa.gov*
Received July 23, 2007, Accepted October 5, 2007

Microcalorimeters with metallic magnetic sensors show great promise for use in astronomical x-ray spectroscopy. We describe the design and fabrication of a lithographically patterned magnetic microcalorimeter. A paramagnetic AuEr film is sputter-deposited as the sensor, which is coupled to a low noise SQUID via a meander superconducting pickup loop used as an inductor. This inductor also provides the magnetic field bias to the sensor. The AuEr film is deposited over this meander such that the field created by a large current flowing in the loop magnetizes the sensor material. The use of thin film techniques in the fabrication of these magnetic sensors not only allows strong magnetic coupling between the sensor and the inductor, it also is scalable for array fabrication.
PACS numbers: 07.85.Fv, 85.25.Oj, 95.55.Ka.

1. INTRODUCTION

A metallic magnetic calorimeter (MMC) consists of an x-ray absorber which is thermally coupled to a material with a temperature dependent magnetization, *M(T)*, at temperatures of the order of 50 mK. The magnetic material acts as a thermometer that senses the temperature rise of the absorber when it absorbs an x-ray photon. Fig. 1(a) shows the essential elements and basic principles of a magnetic calorimeter. A small magnetic field is required to produce a magnetization of the paramagnetic system. Changes in magnetization of the sensor caused by x-ray absorption are

measured through a dc superconducting quantum interference device (SQUID) magnetometer, which can be either directly flux coupled, or transformer coupled, to the sample. MMCs have primarily used erbium, Er^{3+} diluted in gold (AuEr) as the sensor material. Metallic hosts are employed because the interaction of the conduction electrons with the paramagnetic ions can lead to short relaxation time.

Recent results in a single pixel MMC shows 2.7 eV energy resolution for 5.9 keV x-rays using an Er-doped Au paramagnetic sensor coupled to a SQUID[1]. This result demonstrates the potential of this technology. In this experiment, circular disks were cut from the AuEr foil and placed, by hand, in the SQUID loop of a magnetometer. Such a method of assembling is unsuitable for building large arrays of detectors. It is therefore essential to develop fabrication techniques to build large MMC arrays, where each pixel, consisting of a sensor and absorber, can be easily coupled to a SQUID.

2. DETECTOR DESIGN AND FABRICATION

Our devices are built using layers of thin Nb films. The circuit, which is based on a self-inductance concept[2], is shown in Fig. 1(b). A thin layer of AuEr is deposited on a meander superconducting pickup loop, which acts as an inductor. Current applied to the pickup loop produces a magnetization in the AuEr that depends on temperature. A transformer with a mutual inductance to the SQUID input loop is used to null the current passing through the SQUID input coil. The value of the mutual inductance is determined from the constancy of net flux threading through a superconducting loop. When an x-ray is absorbed, the temperature and hence the magnetic susceptibility of the sensor are changed. Consequently, the self-inductance of the pickup loop and the current sensed by the SQUID are also changed. The signals are coupled from the pickup loop to the SQUID through superconducting striplines to minimize stray inductance. Compared to more traditional MMCs, self-inductance MMCs require much thinner magnetic films, eliminate the need for a separate magnetic field for the magnetic sensors, and provide a stronger coupling between the spins and the pickup loop due to their proximity. In addition, in this configuration, the magnetic crosstalk between pixels in an array is also reduced significantly.

The MMC arrays are fabricated with conventional semiconductor processing techniques. Patterning was performed with a contact mask aligner. Four-inch, 500μm thick, single-side polished silicon wafers were used. A layer of thin aluminum oxide (Al_2O_3) was deposited on the silicon substrate as etch stops, while the pickup loops and transformer coils are magnetron-deposited Nb. The loops and coils are patterned using reactive ion etching (RIE) in a single parallel plate etcher, using photoresist as the

etching mask. An electron beam deposited Al_2O_3 film was used to insulate the sensor AuEr film from the Nb pickup loop. Since Al_2O_3 is immune to fluorine chemistry, this layer also serves as the etch stop for washer etching of the transformers. Patterned superconducting micro striplines are utilized in this circuit to minimize stray inductance. Vias capable of carrying high critical current are used for contact wiring between different layers.

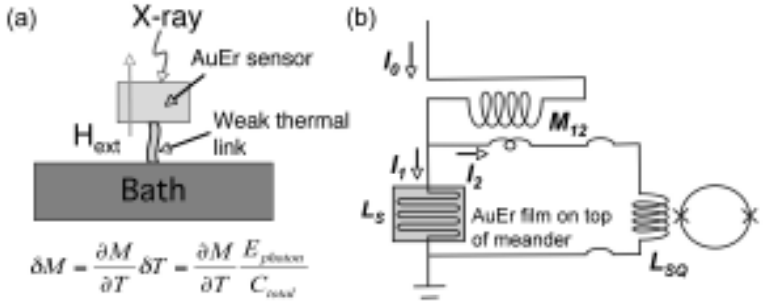

Fig. 1. (a) Essential components and principles of measurement of a metallic magnetic x-ray calorimeter. (b) A schematic diagram of a self-inductance magnetic calorimeter. When an x-ray photon is absorbed in the calorimeter, the change in magnetization of the sensor changes the self-inductance L_s of the meander pickup loop, and consequently induces a change in the current sensed by the SQUID. A transformer with mutual inductance M_{12} is used to null the bias current going into the SQUID input coil.

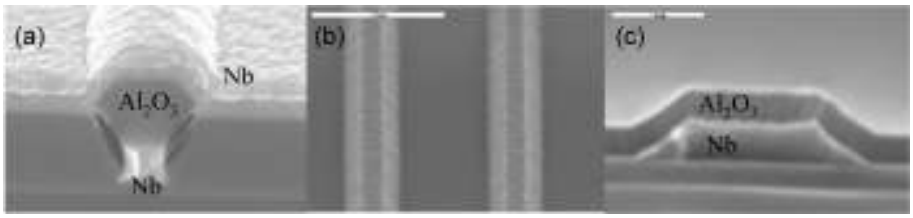

Fig. 2. (a) (Side view) Nb structure etched in a CF_4 and N_2O gas mixture shows a steep slope, and the insulating layer Al_2O_3 suffers from poor step coverage. (b) (Top view) Nb structure etched in a SF_6 and O_2 gas mixture shows a sloped sidewall. (c) (Side view) Al_2O_3 deposited on top of the ramp-edged Nb structure shows conformal coverage and no void formation.

Fig. 2(a) is a cross-sectional scanning electron microscopy image of an insulating Al_2O_3 layer, sandwiched between 2 Nb layers. The bottom layer of Nb is RIE etched in a gas mixture of CF_4 and N_2O, which generates nearly vertical sidewalls, therefore, Al_2O_3 film deposited on top of this feature suffers from shadowing effects. This results in an "overhang" at the top and a "void" at the bottom of the step structures. A thick insulating layer

is therefore necessary to ensure the proper circuit isolation.

To mitigate the shadowing effect, a gas mixture of SF_6 and O_2 was used to produce sloped sidewalls. Adding O_2 to the SF_6 enhances the etch rate of the resist and thereby produces a sloping profile by resist erosion. The thickness of the resist has to be optimized to get the desired slope angle. In addition, plasma parameters in the reactor, such as the chamber pressure, rf power, reactant gas flows, etc., are also found to affect the sidewall profile. Fig. 2(b) shows the etched Nb structure with ramped edges using the SF_6 and O_2 etchant. Fig. 2(c) shows that, with the ramped edge of Nb structure, the step coverage of the Al_2O_3 film is more conformal and void-free. This etching technique enables us to use thinner insulating layer between the pickup loop and AuEr sensor, thus permitting stronger coupling between the sensor spins and the pickup loop.

For the magnetron-sputtered sensing material, two different sensor materials were used: gold doped with 1050 ppm natural Er, (Er with a naturally occurring isotopic distribution), and gold doped with 900 ppm isotopically enriched Er, which will improve detector performance.[3] The deposition was done at room temperature and a very thin layer of Nb is deposited as the binding layer to prevent the AuEr film from peeling off the substrate during lift-off. Ti/Au, deposited by electron beam evaporation, provides a heat sink layer for the sensor.

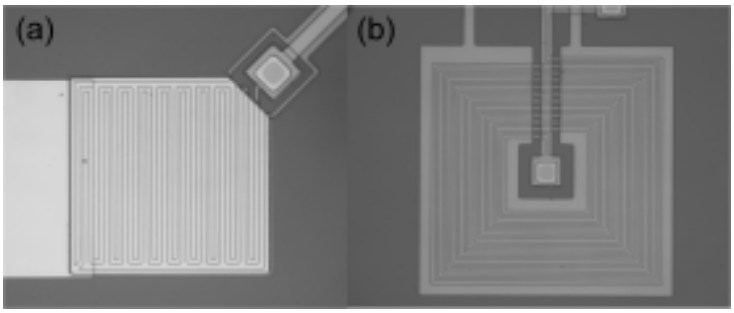

Fig. 3. (a) A 100 μm × 100 μm meander pickup loop with 2 μm wide thin film Nb wires at a 5 μm pitch. A 500 nm thick AuEr film is deposited over the pickup loop. The return current lead of the meander is split to minimize the stray magnetic pickup. (b) Micrograph of the superconducting planar transformer consists of an Al_2O_3 insulating layer, sandwiched between a Nb coil layer and a Nb washer layer. A via in the center provides corssover between the 2 Nb layers.

Fig. 3(a) shows the meandering configuration of the pickup loop, and an AuEr film is deposited on top of it. The loop return lead is split into two to minimize the stray magnetic pickup[3]. Fig. 3(b) shows the

superconducting planar transformer, which ensures that the SQUID is not exposed to large field. The slotted washer is situated in the upper Nb layer[4]. For both the pickup loop and the transformer, the Nb coil line width is 2 μm, and the pitch is 5 μm. The typical critical current density is ~ 12×10^6 A/cm^2 for 200 nm thick Nb at 4.2K. In the prototype MMC arrays, each array consists of 4 pixels, each with an independent SQUID readout, (off chip). An on-chip filter for the detector bias minimizes radio frequency noise, and an on-chip Johnson noise thermometer was also used to monitor the temperature of the chip.

3. RESULTS AND DISCUSSION

The magnetization vs temperature curve of the sputter-deposited AuEr film is shown in Fig. 4. The resulting film is sputtered with an AuEr target with 1050 ppm natural Er. The magnetization is measured in a field of 5 T from room temperature down to 5 K (left figure); and in a field of 500 G for temperature lower than 5 K (right figure). For comparison, the magnetization of the target material is also shown. The Er concentration of the resulting film is determined by the least-square fit using the crystal field parameters[5]. Our sputtered film shows substantially smaller Er concentration than that of the target material, the cause of which is still being investigated.

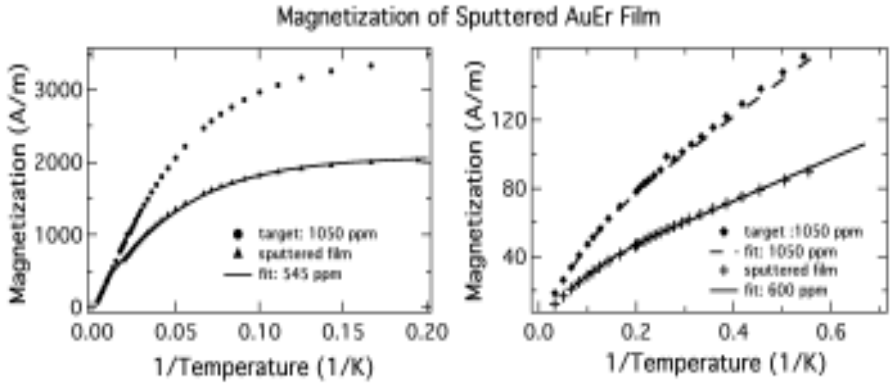

Fig. 4. The magnetization vs temperature curve of the sputtered AuEr film, and of bulk material with 1050 ppm natural Er, measured at 5 T. The sputtered AuEr film has an Er concentration significantly less than that of the target material. The right figure shows the magnetization curves at lower temperatures, measured at 500 G.

To enhance the sensor performance, 900 ppm isotopically enriched AuEr film was used. For these prototype detectors, baseline sensitivity of 5

eV at 5.9 keV x-ray was derived from integrating the noise equivalent power. Details of detector performance, device characterization, and the use of low noise SQUIDs developed at PTB-Berlin, are reported elsewhere[6].

In summary, we have demonstrated a fabrication technique for MMC arrays, based entirely on thin-film technology. Prototype devices of 4 pixel arrays are fabricated and tested with reasonable energy sensitivity in the soft x-ray energy range. We also introduced an etching technique to controllably produce Nb structures with sloped sidewall. Al_2O_3 film deposited on top of these structures can then be made to form a conformal coverage, without overhangs and voids. This technique also enables us to use thinner insulating layer between the spins in the sensor and the Nb pickup loop, thus allowing a stronger coupling between them.

Magnetization measurement of the sensor film, however, indicates an Er concentration on the deposited film different from that of the target material, the cause of which is still under investigation. We have planned further investigation on sputter-deposited AuEr films with controlled Er concentration in order to better control sensor magnetization and to optimize device responses. More MMC detector arrays are being fabricated with the new RIE technique, and with addition of a separate x-ray absorber, which has not been implemented in the early prototype MMC arrays. We also plan to incorporate electroplated Au absorbers into the MMC detectors in the future[7]. This is expected to give us much better quantum efficiency (> 95%).

REFERENCES

1. L. Gastaldo, M. Linck, S. Schafer, H. Rotzinger, A. Burck, S. Kempf, J. Porst, A. Fleischmann, C. Enss, and G. Seidel, this proceeding.
2. B. L. Zink, K. D. Irwin, G. C. Hilton, D. P. Pappas, J. N. Ullom, and M. E. Huber, *Nucl. Instrum. Methods Phys. Res. A* **520**, 52, (2004).
3. A. Fleischmann, C. Enss, and G. Seidel, *Metallic Magnetic Calorimeters* in *Cryogenic Particle Detection*, Ed. C. Enss. Springer (Berlin, 2005).
4. J. M. Jaycox and M. B. Ketchen, *IEEE Trans. on Magnetics*, **MAG-17** (1), 400, (1981).
5. A. Fleischmann, J. Schonefeld, J. Sollner, C. Enss, J. A. Adams, S. R. Bandler, Y. H. Kim, and G. M. Seidel, *J. Low Temp. Physics,* **118**, 7, (2000).
6. H. Rotzinger, J. Adams, S. Bandler, J. Beyer, H. Eguchi, E. Figueroa-Feliciano, W. Hsieh, G. M. Seidel, and T. Stevenson, this proceeding.
7. A. Brown, S. Bandler, R. Brekosky, J. Chervenak, E. Figueroa-Feliciano, F. Finkbeiner, N. Iyomoto, R. L. Kelley, C. A. Kilbourne, F. S. Porter, S. Smith, T. Saab, and J. Sadleir, this proceeding.